



# Experimental Study on Coal Permeability and Damage Evolution Under the Seepage-Stress Coupling

Fujin Lin<sup>1,2</sup>, Guangli Huang<sup>2</sup>, Deyi Jiang<sup>1\*</sup>, Yi He<sup>3</sup> and Jinyang Fan<sup>1\*</sup>

<sup>1</sup>State key laboratory of coal mine disaster dynamics and control, Engineering, Chongqing University, Chongqing, China, <sup>2</sup>China Coal Technology Engineering Group Chongqing Institute, Chongqing, China, <sup>3</sup>School of Metallurgy and Materials Engineering, Chongqing University of Science and Technology, Chongqing, China

In order to study the damage evolution law of coal under the seepage-stress coupling, this paper adopted the rock servo triaxial test system to conduct permeability test for full stress-strain process on 10 sets of coal specimens using steady-state method under different confining pressure and osmotic pressure. The results show that coal permeability has a small fluctuation before the stress peak, and the permeability increases substantially after the peak. The relationship between the plastic damage variable of coal and the equivalent plastic strain is proposed. The research will provide a theoretical basis for hydraulic fracturing gas drainage reservoir.

## OPEN ACCESS

### Edited by:

Alexandre Chemenda,  
UMR7329 Géoazur, France

### Reviewed by:

Huihua Peng,  
Hunan Institute of Engineering, China  
Chao Qin,  
Guizhou University, China

### \*Correspondence:

Deyi Jiang  
deyij@cqu.edu.cn  
Jinyang Fan  
149026673@qq.com

### Specialty section:

This article was submitted to  
Geohazards and Georisks,  
a section of the journal  
Frontiers in Earth Science

**Received:** 02 January 2022

**Accepted:** 22 February 2022

**Published:** 08 April 2022

### Citation:

Lin F, Huang G, Jiang D, He Y and  
Fan J (2022) Experimental Study on  
Coal Permeability and Damage  
Evolution Under the Seepage-  
Stress Coupling.  
Front. Earth Sci. 10:847392.  
doi: 10.3389/feart.2022.847392

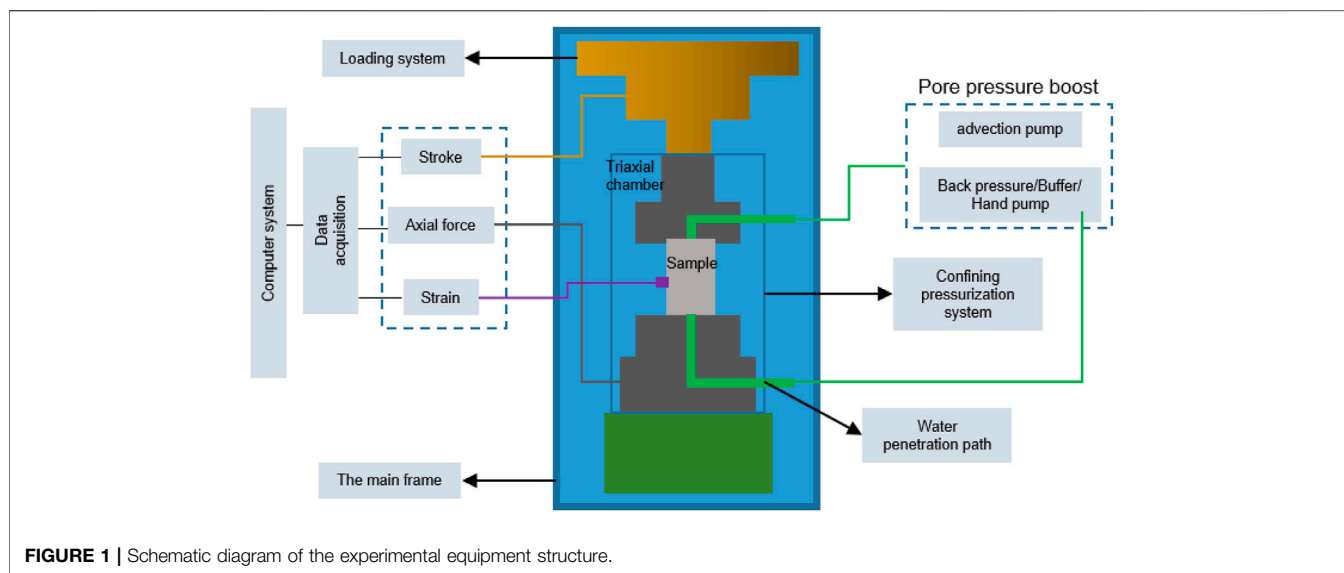
**Keywords:** coal damage, equivalent plastic strain, seepage-stress coupling, permeability, experiment research

## INTRODUCTION

China has a large amount of coalbed methane resources, but the occurrence conditions are complicated, and the permeability of coal seam is generally low, especially in high gas and outburst mines where 95% of mined coal seams are belong to permeability coal seams (Fan et al., 2020a; Liu, 2020a; Liu et al., 2021a; Lu, 2021; Liu et al., 2022). Hydraulic fracturing is a common technical means to increase permeability in coalbed methane extraction. It not only realizes the efficient development of coalbed methane resources, but also provides safety guarantee for coal mine production (Wang et al., 2017; Fan et al., 2019; Liu et al., 2021b). At present, low and even ultra-low permeability of soft coal seams lead to the problems such as low engineering success rate, high development cost, and low single well output, which restricts the large-scale development and utilization of coalbed methane (Fan et al., 2018; Fan et al., 2020b; Kang et al., 2021).

In the oil and shale gas industry, regarding the development, extension and expansion of fractures in rocks, scholars have conducted a lot of experimental studies on how to increase permeability in hydraulic fracturing (Liu, 2020b; Liu, 2020c; Ma, 2021; Xu et al., 2022), and studied influencing factors of hydraulic fracturing under various physical properties and structure characteristics (Liu, 2020d; Zhang, 2021). Detournay (Detournay, 2004) and Wu Pengfei (Wu et al., 2018) studied rock fracture propagation under hydraulic fracturing by means of analytical solution and numerical simulation respectively. In underground coal mines, many useful attempts have been made with hydraulic fracturing technology in order to prevent spontaneous combustion, and roof management (Huang et al., 2007; Jiang et al., 2021; Li et al., 2021; Sun et al., 2021; Zheng, 2021).

In recent years, based on the seepage-damage theory, Chen Mingyi (Chen, 2017) used triaxial permeability tests to study the law of moisture adsorption to coal, the mechanical characteristics,



and the evolution law of permeability and damage. Wang Xiangyu, Zhou Hongwei, et al. (Wang et al., 2018) analyzed the energy change law and permeability characteristics during the deep coal damage process under triaxial cyclic loading. The results show that coal damage is an energy-consuming damage process (Li et al., 2015; Wang et al., 2016; YundongShou et al., 2020). Under different confining pressures, permeability and damage variables present a good exponential function relationship. These studies are mainly based on coal seam water inrush (Rui et al., 2018; Gu et al., 2020). For coal seam gas development projects, the evolution of coal permeability and damage variables due to hydraulic fracturing and permeability improvement technology still needs further research. In particular, the correlation between the plasticity variable and the damage variable and the permeability value after the hydraulic fracturing coal body of the soft coal seam is damaged is studied, the important point is to find the damage evolution equation of plastic strain and form the relationship expression between soft coal damage and permeability.

In this paper, the seepage-stress coupling experiment is used to study the evolution law of coal deformation and permeability during the full stress-strain loading process. The damage evolution equation of coal with equivalent plastic strain under multi-field coupling is established, and the relationship expression between soft coal damage and permeability is proposed.

## TEST DEVICE

The TAW-1000 servo hydraulic triaxial testing machine with 2PB00C advection pump was used in the experiment. The three-axis experimental pressurized loading system is composed of a self-balancing piston, a pressure chamber cylinder, a safety ring and a fixed shoe, a pressure chamber base and a trolley, and an

exhaust valve. The confining pressure loading system consists of a Panasonic motor, a reducer, a flushing pump, and a fuel tank. The pressure sensor is attached to the rigid host, the pressure during the loading process can be tested by the sensor, and the strain gauge is used to measure the radial strain of the specimen. The structure diagram of the test system is shown in **Figure 1**.

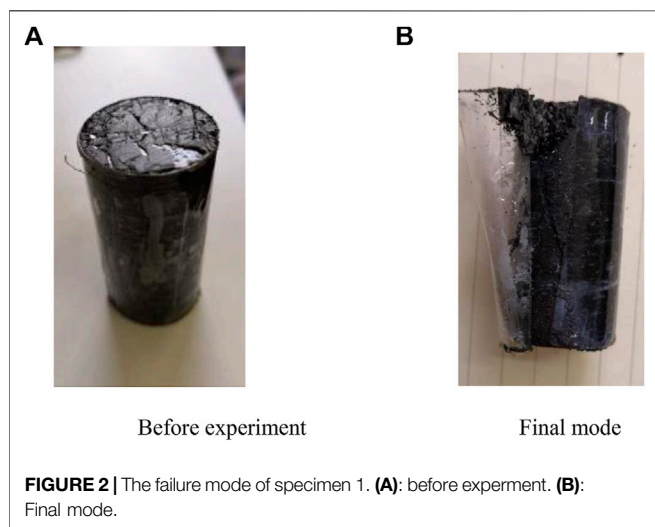
The original coal samples of Shihao Coal Mine in Songzao mining area were taken and made into standard specimens according to the sample preparation method, and uniaxial, triaxial and permeability experiments were carried out to study and analyze the failure form, fracture development and permeability of soft coal under different stress states and osmotic pressures. The seepage characteristics lay the foundation for the study of the damage seepage characteristics of soft coal under seepage-stress coupling. Different confining pressures, inlet pressures and outlet pressures were used to conduct seepage-stress coupling experiments. The dimensions and loading conditions of the test specimens are shown in **Table 1**.

## EXPERIMENTAL RESULTS

The multi-field coupling seepage test system of coal and rock enhanced water injection is sensitive to temperature. In order to minimize the influence of temperature on the experimental results, the test chamber temperature was strictly controlled at  $20 \pm 0.5^\circ\text{C}$ . The specific method for the whole-process stress and strain seepage test of coal and rock is as follows: according to the experimental design, first apply a certain axial pressure  $P_1$ , confining pressure  $P_2$  and pore pressure  $P_3$  (always maintain  $P_2 > P_3$ , otherwise the heat shrinkable plastic and other seals will fail and the experiment will fail), so that water seeps through the specimen. The hydraulic system of the penetration test is servo controlled. The whole experimental process is controlled by a computer, including data acquisition and processing. The specimen axial

**TABLE 1** | Dimensions and loading conditions of test specimens.

Number	Diameter (mm)	Height (mm)	Confining pressure (MPa)	Water inlet pressure (MPa)	Water outlet pressure (MPa)
1	23.68	49.98	8	6	2
2	23.84	50.01	9	6	2
3	23.96	50.03	10	6	2
4	23.78	49.97	11	6	2
5	24.01	49.97	12	6	2
6	23.74	49.63	9	8	2
7	23.71	50.01	9	7	2
8	23.56	49.70	9	5	2
9	23.48	50.01	9	6	1
10	23.89	50.07	9	6	3



deformation and the change process of the osmotic pressure difference over time are measured while applying each level of axial pressure. Read the axial strain and permeability values under each level of axial pressure to plot the stress-strain and permeability-strain relationship curves.

### The Specimen Failure Mode

Part of the specimens before the test, the final failure mode are shown in **Figure 2**.

The final failure simplified model are shown in **Figure 3**. According to different damage types, it can be roughly divided

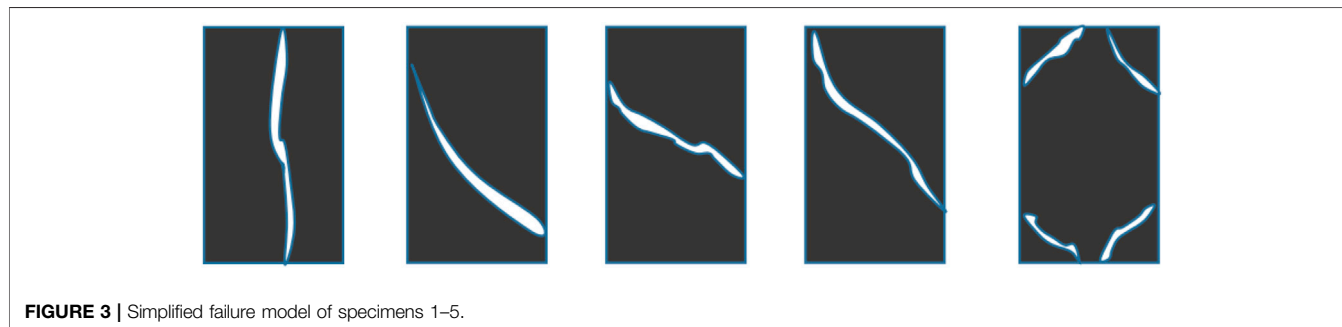
into axial center type, 30° shear type, 45° shear type, irregular shear type, and symmetrical edge destructive type.

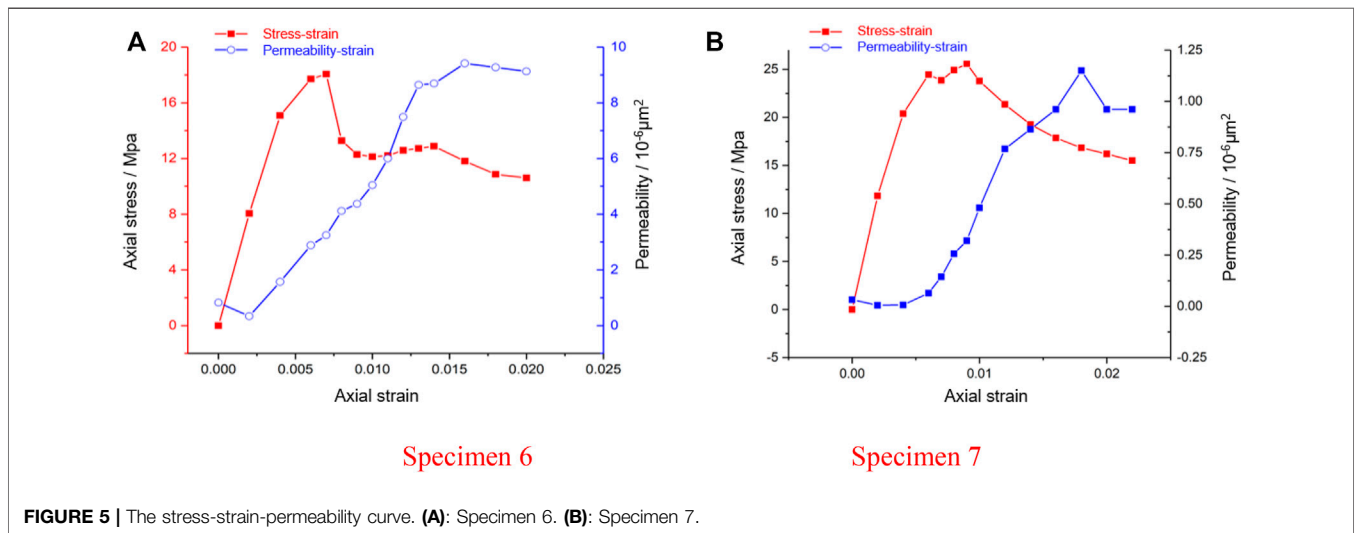
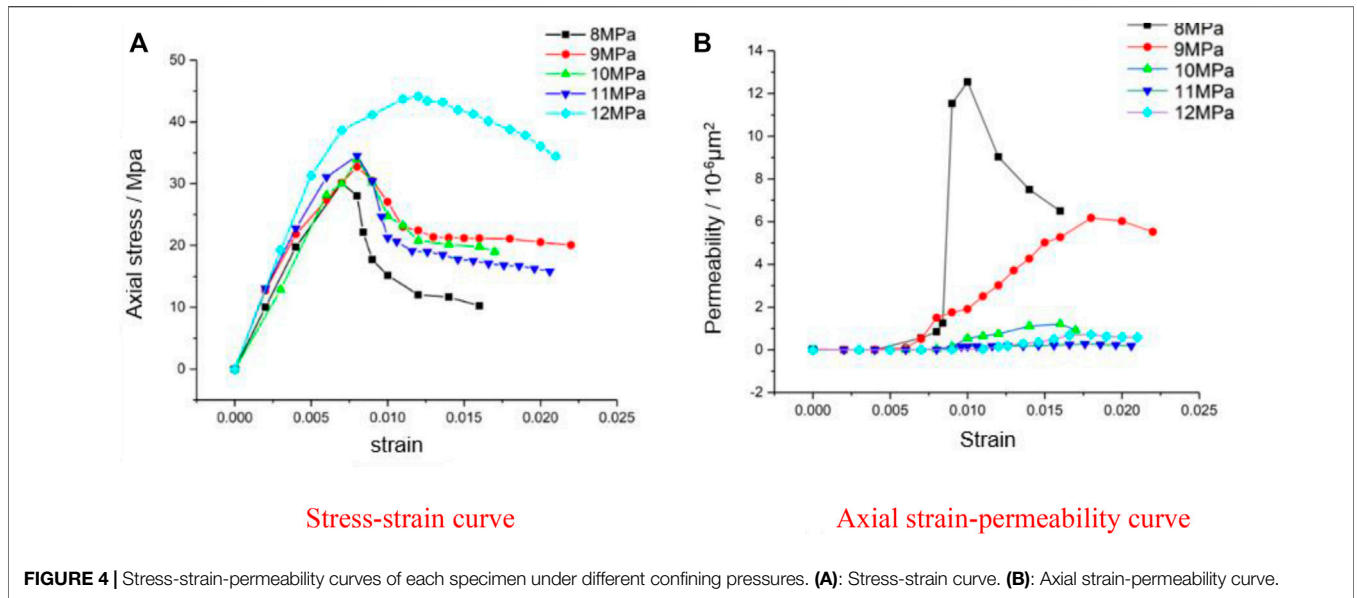
According to the experiment results, the initial defects and strength of raw coal have great discreteness and are relatively typical heterogeneous material, leading to different failures of various specimens, which is also the difficulty in quantitative study on the variation rules of parameters such as damage and permeability of coal and rock specimens.

### The Influence of Confining Pressure

The experiment adopts stable Darcy seepage flow to determine the permeability of the coal sample, that is, the permeability is calculated based on the measurement parameters such as the flow rate of the fluid passing through the coal sample in a unit time and the osmotic pressure difference between the two ends of the coal sample. **Figure 4** show the axial stress-axial strain and axial strain-permeability curves of each specimen.

It can be seen from the experiment results that confining pressure has a great impact on the permeability and deformation of the coal and rock specimens under the seepage-stress coupling during the whole stress-strain process. Under confining pressure, coal and rock has higher strength. As the confining pressure increases, the modulus of elasticity of coal and rock also increases. For its reason, the pore crack (damage) in coal is reduced under confining pressure, the presence of confining pressure during compression inhibits lateral displacement, making it more difficult for the rock to break. The permeability of coal and rock fluctuates to a certain extent before the stress peak. After the stress reaches the peak, there will be a “sudden jump”, and the





peak permeability always appears after the peak of strain, showing the characteristic of “hysteresis”. This phenomenon is related to the failure of the specimen. After the stress peak, the specimen is damaged, and the seepage has a “sudden jump” change.

### The Influence of Osmotic Pressure

Figure 5 show the stress-strain-permeability curves of some specimens. Figure 6 shows the permeability curves under different pore pressures. It can be seen from the experimental results that under the same confining pressure and different osmotic pressures, the stress, strain and permeability of coal and rock display the following laws:

With the increase of osmotic pressure, the initial permeability, minimum permeability and maximum permeability of coal increase. When the osmotic pressure increases, the multiple of permeability decrease becomes

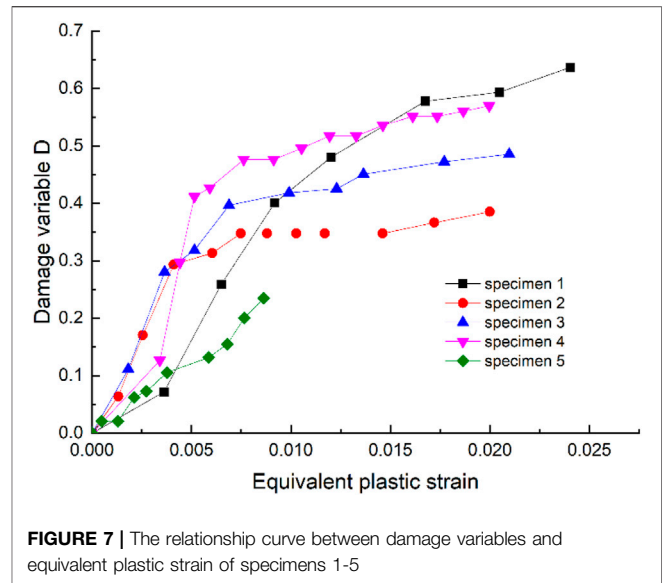
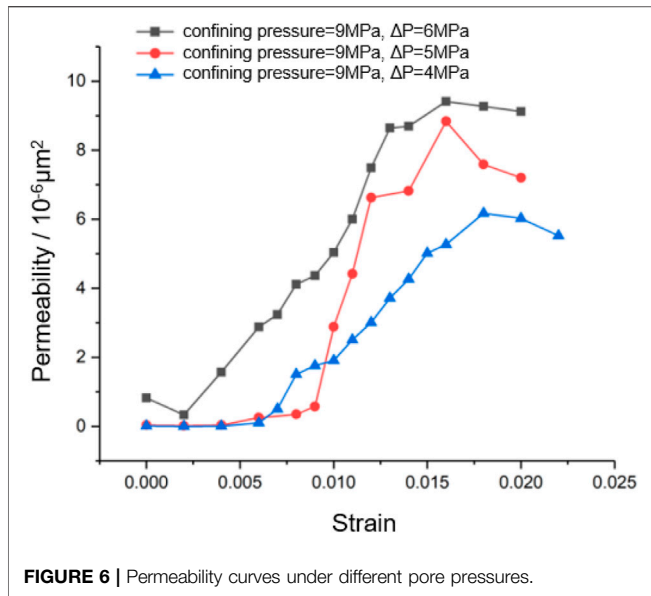
smaller in the compaction stage. The increase in osmotic pressure difference reduces the residual stress after the peak and weakens the coal and rock.

The strength of coal itself and the original damage have a great influence on the permeability. The lower the specimen strength, the easier it is to damage. The greater the original damage, the greater the permeability.

### LAW OF DAMAGE EVOLUTION

#### Equivalent Stress and Equivalent Plastic Strain

Based on the theory of plastic mechanics, the equivalent stress  $\sigma_1$  is required to study the material yield under complex stress states, which is defined as follows (Li, 2020):



$$\sigma_i = \frac{1}{\sqrt{2}} [(\sigma_1 - \sigma_2)^2 + (\sigma_2 - \sigma_3)^2 + (\sigma_3 - \sigma_1)^2]^{\frac{1}{2}} \quad (1)$$

Where,  $\sigma_1$ ,  $\sigma_2$ ,  $\sigma_3$  are the first principal stress, the second principal stress and the third principal stress, respectively. The equivalent strain  $\epsilon_i$  corresponding to the equivalent stress is defined as:

$$\epsilon_i = \frac{\sqrt{2}}{3} [(\epsilon_1 - \epsilon_2)^2 + (\epsilon_2 - \epsilon_3)^2 + (\epsilon_3 - \epsilon_1)^2]^{\frac{1}{2}} \quad (2)$$

Where,  $\epsilon_1$ ,  $\epsilon_2$ ,  $\epsilon_3$  are the first principal strain, the second principal strain and the third principal strain, respectively. Since the total strain can be regarded as the sum of elastic strain and plasticity, the equivalent plastic strain  $\epsilon_i^p$  can be expressed as:

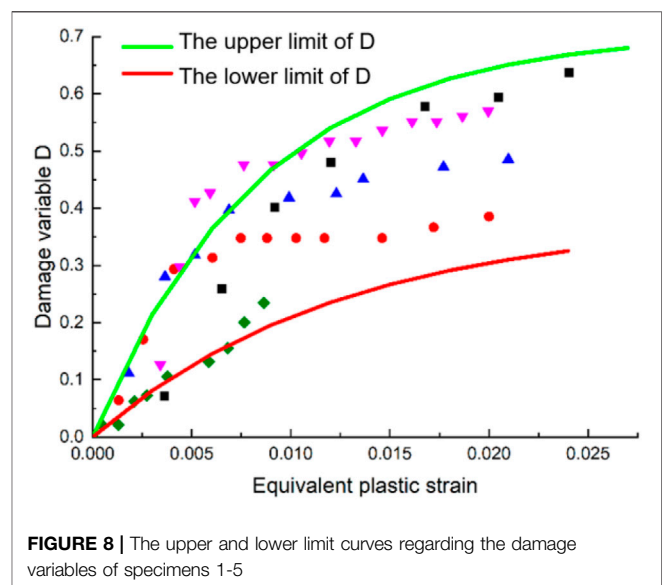
$$\epsilon_i^p = \epsilon_i - \epsilon_i^e \quad (3)$$

Where,  $\epsilon_i^e$  is the equivalent elastic strain.

### Experimental Results of Plastic Damage Evolution

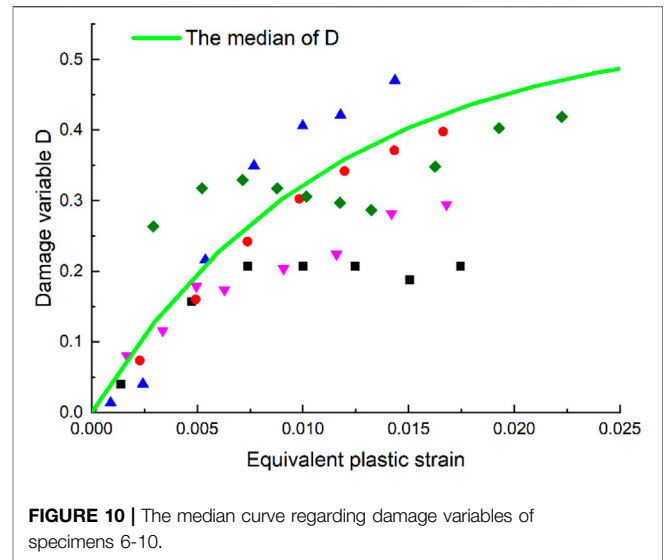
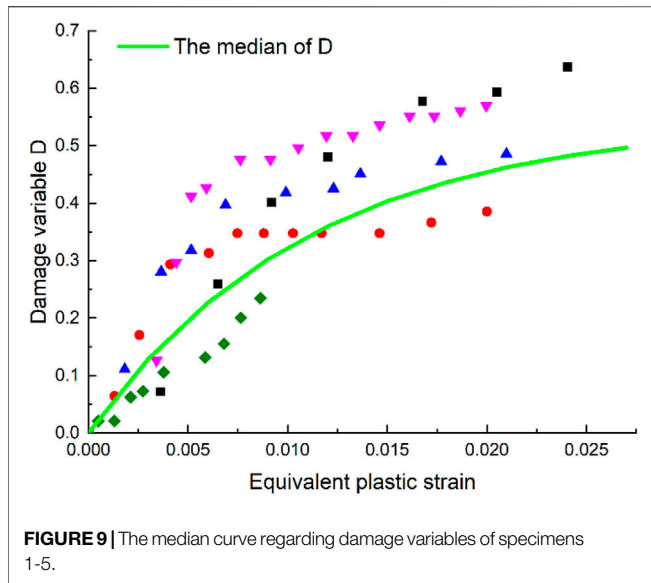
Based on the results of this experiment, it can be considered that the damage in the elastic deformation stage of coal and rock mass is negligible. After entry into the plastic stage, due to the presence of defects such as heterogeneous properties and microscopic pores, the effective bearing area of coal and rock will gradually decrease with increase in plasticity. It can be considered that the damage of coal and rock mass starts from the plastic stage. To this end, the following hypotheses are made:

- 1) The effective bearing area of coal and rock does not change in the elastic stage, that is, no damage occurs, and the damage variable is 0;
- 2) The occurrence and evolution of damage are only related to plastic deformation, which can be described by equivalent plastic strain.



Based on the above hypotheses, equations (1)~(3) can be used to plot the relationship curve between the damage variable and the equivalent plastic strain of each specimen in this experiment. Among them, the basic definition form of the elastic modulus method is used as the method for calculating the damage degree value. The loading conditions of specimens 1-5 include fixed inlet and outlet water pressure and changed confining pressure. The relationship curve between the damage variable and the equivalent plastic strain is shown in **Figure 7**.

Due to the heterogeneous nature of coal and rock materials, it can be seen from **Figure 9** that the coal-rock fluid-solid coupling experiment data is relatively discrete when the confining pressure is changed. This is different from the previous hypothesis that the damage occurrence and evolution is only related to plastic deformation.



By analyzing the experimental data of each specimen, it is found that there is a change law in which the damage variable first increases rapidly with the equivalent plastic strain, and then tends to a fixed value. The damage variable  $D$  can be fitted with the following formula:

$$D = A_0 \exp(-A_1 \varepsilon_i^p) + A_2 \quad (4)$$

According to the definition of plastic damage, when the equivalent plastic strain is  $\varepsilon_i^p = 0$ ,  $D = 0$ , then Eq. 4 can be rewritten as:

$$D = A_0 [\exp(-A_1 \varepsilon_i^p) - 1] \quad (5)$$

The parameters  $A_0$ ,  $A_1$  in the formula are related to the maximum equivalent plastic strain at material failure, the critical damage variable at failure, and other material properties. The lower limit and upper limit of the damage variable of specimens 1-5 are shown in Figure 8. The upper and lower limits are respectively expressed as:

$$D = 0.71 [1 - \exp(-120 \varepsilon_i^p)] \quad (6)$$

$$D = 0.38 [1 - \exp(-80 \varepsilon_i^p)] \quad (7)$$

In this fluid-solid coupling experiment, the experimental data showing the change in damage variable of the coal body with the equivalent plastic strain is somewhat discrete. However, the results of specimens 1-5 are basically distributed within the upper and lower limits of the damage variable in Eqs 6, 7. Based on the expression of the upper and lower limits of the coal body damage variable, the median can be expressed as:

$$D = 0.54 [1 - \exp(-90 \varepsilon_i^p)] \quad (8)$$

It can be seen from Figure 9 that the experimental results of specimens 1-5 are basically distributed around the curve of Eq. 8. For loading conditions of specimens 6-10, fixed confining pressure is 9 MPa, and the water pressures at the inlet and

outlet are different. The change of the damage variable with the equivalent plastic strain is shown in Figure 10.

According to Figures 9, 10, due to the heterogeneous characteristics of the coal and rock specimens, it can be considered that the damage evolution law of the coal and rock specimens within the scope of this experiment can be described by Eq. 8.

## LAW OF SEEPAGE EVOLUTION

Coal is a typical non-uniform porous medium material. When the external load is relatively small, that is, when the overall coal body is still in the elastic stage, the permeability change can be described by the change of porosity or volumetric strain. According to the seepage cube law, it can be expressed as:

$$K = K_0 (1 + \varepsilon_v)^3 \quad (9)$$

When the stress reaches a certain strength, the microvoids and cracks inside the coal body will expand and converge, followed by initial damage. As the loading progresses further, the damage continues to increase and the permeability changes greatly. Considering the action of fluid-solid coupling and the effect of damage, if we only take into account the effect of volumetric strain when studying the seepage law, there will be relatively big errors.

In order to consider the damage impact on coal seepage, the concept of “representative voxel (REV)” is used for simplified analysis. Take a cube of sufficient size with any point in the coal body as the center, its cross-sectional area perpendicular to the seepage direction is  $dA$ , the length of the prism parallel to the seepage direction is  $dL$ , the damage variable of the representative voxel during the stress process is  $D$ . The damage is simplified to a cube in the middle of the representative voxel with a height  $dL$  and a bottom area  $DdA$ . Then the damage evolution process of the

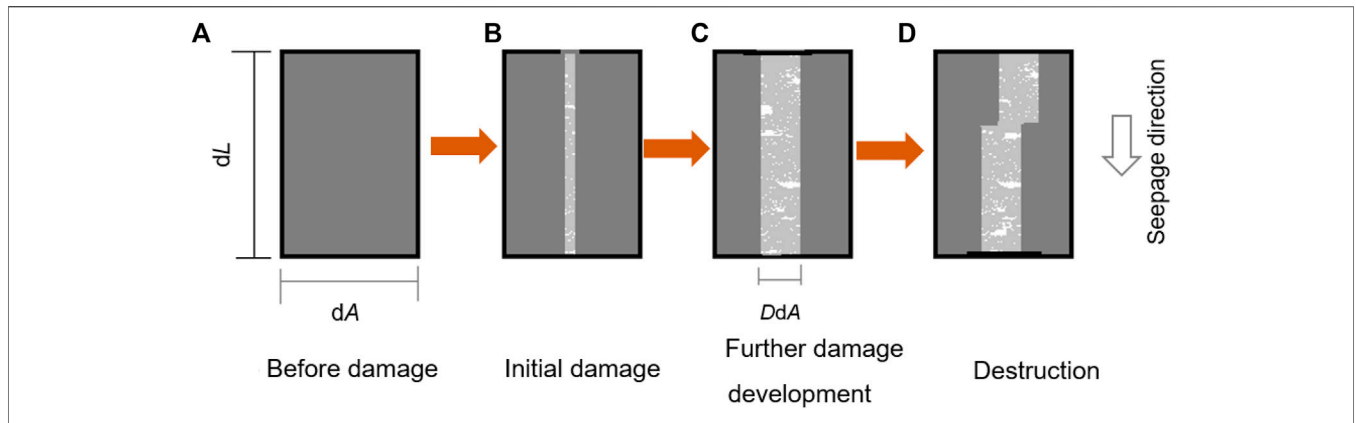


**FIGURE 11** | Damage evolution process of representative voxel. **(A)** Before damage. **(B)** Initial damage. **(C)** Further damage development. **(D)** Destruction.

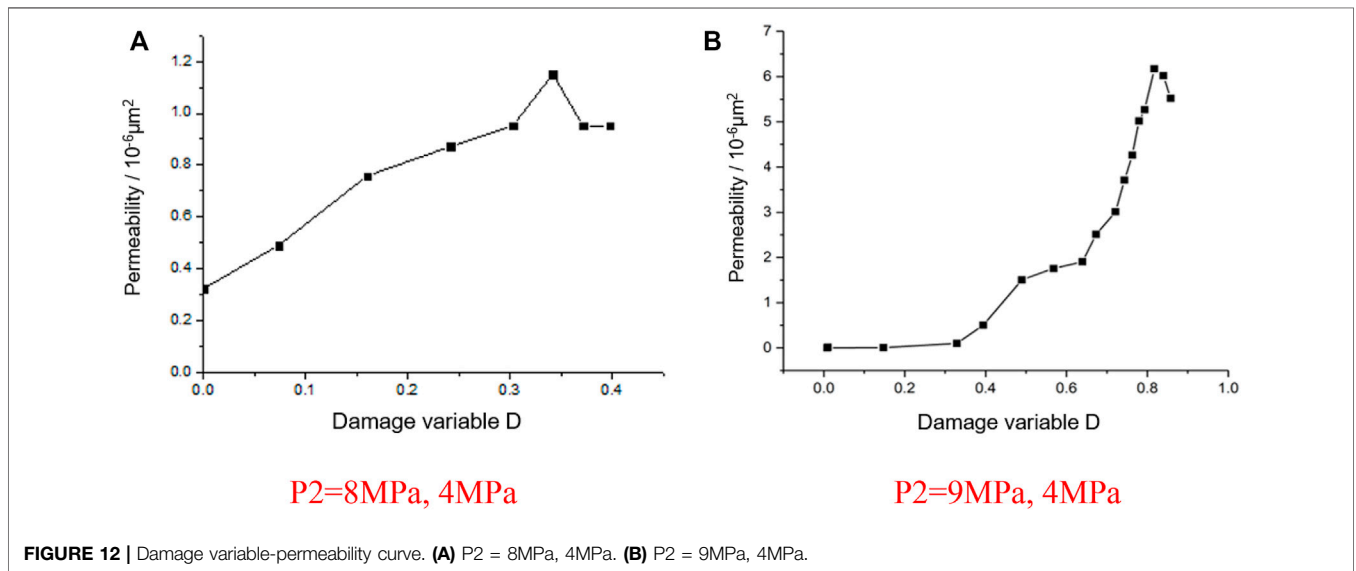


**FIGURE 12** | Damage variable-permeability curve. **(A)** P2 = 8MPa, 4MPa. **(B)** P2 = 9MPa, 4MPa.

representative voxel under the action of fluid-solid coupling can be simplified as shown in **Figure 11**.

As the load increases, damage begins to appear in the coal body. Due to the strong permeability of the damaged area, the permeability of the representative voxel increases; with the further damage development, the increase in permeability of the representative voxel accelerates; when the damage develops to a certain extent, there is smaller increase in damage area, and even changes such as misalignment will occur in the damage area, resulting in a slower increase or even a decrease in the permeability at the later stage of loading.

Based on the above analysis, let the seepage flow rate of the undamaged part of the representative voxel be  $q^M$  and the seepage flow rate of the damaged part be  $q^D$ , then the permeability calculation formula can be expressed as:

$$k = \frac{(q^M + q^D)\mu dL}{dA\Delta P} \tag{10}$$

Where,  $\Delta P$  is the water injection pressure difference between the upper and lower ends of the representative voxel, and  $\mu$  is the water injection viscosity. Considering the cross-sectional area of the undamaged and damaged parts of the representative voxel, the above formula can be further expressed as:

$$k = (1 - D)k^M + Dk^D \tag{11}$$

Where,  $k^M$  and  $k^D$  are the permeability of undamaged and damaged coal. Let  $k_0^M$  and  $k_0^D$  be the initial permeability of undamaged and damaged coal. Considering the cubic law of seepage, there is:

$$k = [(1 - D)k_0^M + Dk_0^D](1 + \epsilon_v)^3 \tag{12}$$

The above equation is changed to the no-dimensional form, then there is:

$$\frac{k}{k_0^M} (1 + \varepsilon_v)^{-3} = 1 + \left( \frac{k_0^D}{k_0^M} - 1 \right) D \quad (13)$$

It can be seen from Eq. 13 that the left end of the equation is the dimensionless penetration that excludes the influence of material volume deformation, and the relationship with the plastic damage variable is the linear relationship of the slope  $\frac{k_0^D}{k_0^M} - 1$ . This formula can basically reflect the law that the permeability of coal and rock materials changes with the change of volumetric strain rate before plastic damage, while after the plastic damage occurs and before the permeability reaches the peak, the permeability increases with the increase of plastic damage. The relationship curves between damage variables and permeability of some specimens in this experiment are shown in Figure 12.

It can be seen from the figure that the results of this experiment basically support Eq. 13, and the experimental data agrees well with the law of equation 2.16.

## CONCLUSION

This paper shows through experimental methods that there is a certain law in permeability evolution during coal and rock failure. The main factors affecting permeability change include the development of fractures, the fracture penetration and failure modes in the process of coal and rock damage evolution. Through the analysis and summary of the experimental data, the following conclusions are drawn:

- 1) Through experimental research, the general law of permeability change of coal and rock in the full stress-strain process is that, in the elastic stage, permeability decreases slightly with the increase of stress; in the closed stage of primary fractures, permeability changes little without primary fracture development; in the elasto-plastic stage, with

the expansion and penetration of new cracks, the permeability of coal first slowly increases and then sharply increases, presenting a “step” phenomenon.

- 2) The permeability of coal and rock is obviously related to the damage and failure state of the rock, which is an external manifestation of the damage and failure state of the coal and rock. The coal permeability evolution process corresponds to the damage and failure state of coal and rock, showing obvious stages, and there are obvious sudden increases in permeability and peak points in the evolution process.
- 3) The damage and destruction of rock under seepage pressure is affected by confining pressure and seepage water pressure. The presence of confining pressure inhibits the damage and fracture of rock mass, and seepage water pressure greatly promotes the damage and fracture of rock mass.
- 4) Through data analysis, the relationship between coal and rock failure, permeability, stress state and volumetric strain during deformation is discovered, and the evolution equation of the plastic damage variable is proposed. Through representative voxel and simplification, the relationship between coal and rock permeability considering damage impact is derived.

## DATA AVAILABILITY STATEMENT

The raw data supporting the conclusion of this article will be made available by the authors, without undue reservation.

## AUTHOR CONTRIBUTIONS

FL: Methodology, Investigation, Software, Editing draft; GH: Writing-review and; editing, Supervision; DJ: Writing-review and, editing, Supervision; YH and JF: Methodology, Investigation, Software, Writing-original draft.

## REFERENCES

- Chen, M. (2017). *Research on the Mechanical Damage and Permeability Evolution Mechanism of Low-Rank Bituminous Coal under Coal-Gas-Water coupling*[D]. Xuzhou: China University of Mining and Technology.
- Detournay, E. (2004). Propagation Regimes of Fluid-Driven Fractures in Impermeable Rocks. *Int. J. Geomech.* 4 (1), 35–45. doi:10.1061/(asce)1532-3641(2004)4:1(35)
- Fan, J., Jiang, D., Chen, J., Liu, W., Tiedeu Ngaha, W., and Chen, J. (2018). Fatigue Performance of Ordinary concrete under Discontinuous Cyclic Loading. *Construction Building Mater.* 166, 974–981. doi:10.1016/j.conbuildmat.2018.01.115
- Fan, J., Jiang, D., Liu, W., Wu, F., Chen, J., and Daemen, J. (2019). Discontinuous Fatigue of Salt Rock with Low-Stress Intervals. *Int. J. Rock Mech. Mining Sci.* 115, 77–86. doi:10.1016/j.ijrmm.2019.01.013
- Fan, J., Liu, P., Li, J., and Jiang, D. (2020). A Coupled Methane/air Flow Model for Coal Gas Drainage: Model Development and Finite-Difference Solution. *Process Saf. Environ. Prot.* 141, 288–304. doi:10.1016/j.psep.2020.05.015
- Fan, J., Liu, W., Jiang, D., Chen, J., Tiedeu, W. N., and Daemen, J. J. K. (2020). Time Interval Effect in Triaxial Discontinuous Cyclic Compression Tests and Simulations for the Residual Stress in Rock Salt. *Rock Mech. Rock Eng.* 53 (9), 4061–4076. doi:10.1007/s00603-020-02150-y
- Gu, Q., Huang, Z., Li, S., Zeng, W., Wu, Y., and Zhao, K. (2020). An Approach for Water-Inrush Risk Assessment of Deep Coal Seam Mining: a Case Study in Xinlongzhuang Coal Mine. *Environ. Sci. Pollut. Res.* 27 (34), 43163–43176. doi:10.1007/s11356-020-10225-0
- Huang, B. X., Liu, C. Y., and Cheng, Q. Y. (2007). “Research on the Technology of Weakening Hard Coal Mass Strength through Hydraulic Fracture,” in *International Symposium on Mining Science and Safety Technology* (PEOPLES R CHINA: Jiaozuo).
- Jiang, D., Li, Z., Liu, W., Ban, F., Chen, J., Wang, Y., et al. (2021). Construction Simulating and Controlling of the two-well-Vertical(TWV) Salt Caverns with Gas Blanket. *J. Nat. Gas Sci. Eng.* 96, 104291. doi:10.1016/j.jngse.2021.104291
- Kang, Y., Fan, J., Jiang, D., and Li, Z. (2021). Influence of Geological and Environmental Factors on the Reconsolidation Behavior of Fine Granular Salt. *Nat. Resour. Res.* 30 (1), 805–826. doi:10.1007/s11053-020-09732-1
- Li, D., Liu, W., Jiang, D., Chen, J., Fan, J., and Qiao, W. (2021). Quantitative Investigation on the Stability of Salt Cavity Gas Storage with Multiple Interlayers above the Cavity Roof. *J. Energ. Storage* 44, 103298. doi:10.1016/j.est.2021.103298
- Li, F. F. (2020). Study of Mechanical Properties of Claystone Based on Plastic Damage. *Rock Soil Mech.* 41 (1), 132–140. doi:10.16285/j.rsm.2018.2177
- Li, S. G., Wang, N., and Zhang, T. J. (2015). “Study on Damage Evolution Characteristics of Coal and Rock Uniaxial Compression Based on the



- Acoustic Emission," in *4th International Conference on Sustainable Energy and Environmental Engineering (ICSEEE)* (Shenzhen: PEOPLES R CHINA).
- Liu, P., Fan, J., Jiang, D., and Li, J. (2021). Evaluation of Underground Coal Gas Drainage Performance: Mine Site Measurements and Parametric Sensitivity Analysis. *Process Saf. Environ. Prot.* 148, 711–723. doi:10.1016/j.psep.2021.01.054
- Liu, P., Fan, L., Fan, J., and Zhong, F. (2021). Effect of Water Content on the Induced Alteration of Pore Morphology and Gas Sorption/diffusion Kinetics in Coal with Ultrasound Treatment. *Fuel* 306, 121752. doi:10.1016/j.fuel.2021.121752
- Liu, P., Liu, A., Liu, S., and Qi, L. (2022). Experimental Evaluation of Ultrasound Treatment Induced Pore Structure and Gas Desorption Behavior Alterations of Coal. *Fuel* 307, 121855. doi:10.1016/j.fuel.2021.121855
- Liu, R. (2020). Statistical Analysis of Acoustic Emission in Uniaxial Compression of Tectonic and Non-tectonic Coal. *Appl. Sciences-Basel* 10 (10), 3555. doi:10.3390/app10103555
- Liu, R. (2020). Tunnel Construction Ventilation Frequency-Control Based on Radial Basis Function Neural Network. *Automation in Construction* 118, 103293. doi:10.1016/j.autcon.2020.103293
- Liu, W. (2020). Research on Gas Leakage and Collapse in the Cavern Roof of Underground Natural Gas Storage in Thinly Bedded Salt Rocks. *J. Energ. Storage* 31, 101669. doi:10.1016/j.est.2020.101669
- Liu, W. (2020). Study on the Mechanical Properties of Man-Made Salt Rock Samples with Impurities. *J. Nat. Gas Sci. Eng.* 84, 103683. doi:10.1016/j.jngse.2020.103683
- Lu, J. L. (2021). Characterization of Full Pore and Stress Compression Response of Reservoirs with Different Coal Ranks. *FRONTIERS EARTH SCIENCE* 9, 764853. doi:10.3389/feart.2021.764853
- Ma, L. H. (2021). Analysis of Damages in Layered Surrounding Rocks Induced by Blasting during Tunnel Construction. *Int. J. Struct. Stab. Dyn.* 21 (07), 21500899. doi:10.1142/s0219455421500899
- Rui, G., Yan, H., Ju, F., Mei, X., and Wang, X. (2018). Influential Factors and Control of Water Inrush in a Coal Seam as the Main Aquifer. *Int. J. Mining Sci. Tech.* 28 (2), 187–193. doi:10.1016/j.ijmst.2017.12.017
- Sun, Y. X., Fu, Y. K., and Wang, T. (2021). Field Application of Directional Hydraulic Fracturing Technology for Controlling Thick Hard Roof: a Case Study. *Arabian J. Geosciences* 14 (6), 438. doi:10.1007/s12517-021-06790-4
- Wang, T., Hu, W., Elsworth, D., Zhou, W., Zhou, W., Zhao, X., et al. (2017). The Effect of Natural Fractures on Hydraulic Fracturing Propagation in Coal Seams. *J. Pet. Sci. Eng.* 150, 180–190. doi:10.1016/j.petrol.2016.12.009
- Wang, Xiangyu., Zhou, Hongwei., Zhong, Jiangcheng., Zhang, Lei., Wang, Chaosheng., and Lu, An. (2018). Energy Evolution and Permeability Characteristics of Deep Coal Damage under Triaxial Cyclic Loading and Unloading[J]. *Chin. J. Rock Mech. Eng.* 37 (12), 2676–2684. doi:10.13722/j.cnki.jrme.2018.0697
- Wang, X., Wen, Z.-j., and Jiang, Y.-j. (2016). Time-Space Effect of Stress Field and Damage Evolution Law of Compressed Coal-Rock. *Geotech. Geol. Eng.* 34 (6), 1933–1940. doi:10.1007/s10706-016-0074-y
- Wu, P., Liang, W., Lian, H., Jiang, Y., Geng, Y., Cao, M., et al. (2018). Mechanism and Experimental Investigation of the Formation of Hydro-Fracture System by Fracturing through the Interface of Large-Size Coal-Rock [J]. *J. China Coal Soc.* 43 (5), 1381–1389.
- Xu, F., Xu, Z., Tang, S., Ren, Q., Guo, Y., Wang, L., et al. (2022). Evolution of Physical and Mechanical Properties of Cementing Materials during Underground Energy Exploitation and Storage. *J. Energ. Storage* 45, 103775. doi:10.1016/j.est.2021.103775
- Yundong Shou, Y. D., Jianwei Zhang, J. W., and Filippo Berto, F. (2020). Experimental and Analytical Investigation on the Coupled Elastoplastic Damage Model of Coal-Rock. *Frattura Ed. Integrità Strutturale* 14 (53), 434–445. doi:10.3221/igf-esis.53.34
- Zhang, X. (2021). Investigation on the Influences of Interlayer Contents on Stability and Usability of Energy Storage Caverns in Bedded Rock Salt. *Energy* 231, 120968. doi:10.1016/j.energy.2021.120968
- Zheng, K. G. (2021). Evolution and Management of Thick-Hard Roof Using Goaf-Based Multistage Hydraulic Fracturing Technology-A Case Study in Western Chinese Coal Field. *Arabian J. Geosciences* 14 (10), 876. doi:10.1007/s12517-021-07111-5

**Conflict of Interest:** The authors declare that the research was conducted in the absence of any commercial or financial relationships that could be construed as a potential conflict of interest.

**Publisher's Note:** All claims expressed in this article are solely those of the authors and do not necessarily represent those of their affiliated organizations, or those of the publisher, the editors and the reviewers. Any product that may be evaluated in this article, or claim that may be made by its manufacturer, is not guaranteed or endorsed by the publisher.

Copyright © 2022 Lin, Huang, Jiang, He and Fan. This is an open-access article distributed under the terms of the Creative Commons Attribution License (CC BY). The use, distribution or reproduction in other forums is permitted, provided the original author(s) and the copyright owner(s) are credited and that the original publication in this journal is cited, in accordance with accepted academic practice. No use, distribution or reproduction is permitted which does not comply with these terms.